ACS APPLIED MATERIALS & INTERFACES

Research Article

www.acsami.org

Nitrogen-Doped Graphene Nanosheets from Bulk Graphite using Microwave Irradiation

Kwang Hoon Lee,[†] Jinwoo Oh,[†,§] Jeong Gon Son,[†] Heesuk Kim,[†] and Sang-Soo Lee*[,†,‡]

[†]Photo-Electronic Hybrids Research Center, Korea Institute of Science and Technology, Seoul 136-791, Korea

[‡]KU-KIST Graduate School of Converging Science and Technology, Korea University, Seoul 136-701, Korea

[§]Department of Polymer Science and Engineering, Inha University, Incheon 402-751, Korea

Supporting Information

ABSTRACT: Using simple microwave irradiation under the presence of sodium amide as a nitrogen source, preparation of nitrogen-doped graphene nanosheets has been successfully demonstrated. It is notable that exfoliation and nitrogen doping of graphite to nitrogen-doped graphene simultaneously occurred during the microwave irradiation within a minute, and nitrogen content of the doped graphene could reach up to 8.1%. It was also found that the binding configuration of nitrogen atom on graphitic layer consisted of various nitrogen-containing moieties such as pyridine-N, pyrrolic-N, and quaternary-N, and their composition was changed as a function of irradiation power. Although formation of undoped reduced graphene oxide by microwave irradiation resulted in slight increase of electrical conductivity because of the reductive recovery of oxidized graphite to graphene, nitrogen doping involved during irradiation induced much more notable increase of electrical conductivity more than 300 S cm^{-1}. Furthermore, nitrogen-doped graphene showed highly enhanced capacitive performance than that of undoped reduced graphene oxide, the specific capacitance of 200 F/g (current density of 0.5 A/g), which ascribes the pseudocapacitive effect from the incorporation of nitrogen atom on graphitic layer.

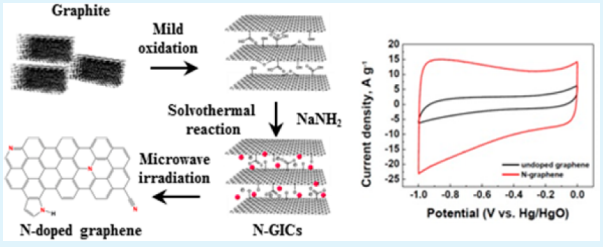

KEYWORDS: *graphene nanosheet, graphite, nitrogen-doped, microwave irradiation*

1. INTRODUCTION

Graphene as a new two-dimensional (2D) macromolecule is of great interest because of the exceptionally high electron mobility and electrical conductivity, uniquely high thermal conductivity in atomic scale, very stiff mechanical properties and gas barrier properties. Thus, the graphene has been widely studied for prospective applications in many fields, including nanoscale-electronics,[1] biosensors,[2] transistors,[3] energy storage materials,[4] and catalysts.[5] However, the lack of electronic bandgap of pristine graphene has been a big hurdle in direct usage for the nanoscale-electronics as a high electronic mobility channel, such as low on/off ratio phenomena of pristine graphene based transistors. To tailor the electronic, chemical and magnetic properties of graphene, especially to open the bandgap of graphene, chemical doping has been considered to be one of the most efficient approaches.[6−8] For the chemical doping of carbon-based materials, nitrogen and boron are general candidates due to the atomic size similarity and valence electrons available to form stable covalent bonds with adjacent carbon atoms, which are both similar to those characteristics of carbon atom and thus, easy to substitute with carbon atoms.[9,10] Especially, nitrogen doping (N-doping) is one of the most effective methods for increasing the chemical reactivity of graphene and tailoring transport behaviors of electron and phonon within graphitic sheet that are correlated with the stronger electronegativity of nitrogen relative to that of carbon, and the conjugation between the lone pair electrons of nitrogen and π-electrons of graphene.

Nitrogen-doped graphene (N-graphene) has been reported to expand widely the explored potential applications, such as higher electrocatalytic activity for the reduction of hydrogen peroxide and oxygen[11] and oxidation of methanol[12] than pristine graphene and better performance in Li ion battery applications.[13] More importantly, incorporating different types of nitrogen into the carbon network would provide the N-doped graphene with more functional groups for property design.[14−16] Thus, many researchers have suggested several methods to produce N-graphene; chemical vapor deposition (CVD) method,[13] arc-discharge method,[17] nitrogen plasma process,[18] thermal annealing with nitrogen source,[19,20] and so on. Nevertheless, most of the methods to prepare doped graphene have exhibited unavoidable disadvantages such as yield of limited scale, long preparation time, and complex procedure coupled with expensive equipment.

This paper includes a novel microwave irradiation approach to produce N-doped few layer graphene from bulk graphite. The microwave irradiation offers great advantages such as simple and fast procedure because selective dielectric heating imparted by

Received: December 13, 2013
Accepted: March 6, 2014
Published: March 6, 2014

   dx.doi.org/10.1021/am405735c | ACS Appl. Mater. Interfaces 2014, 6, 6361−6368

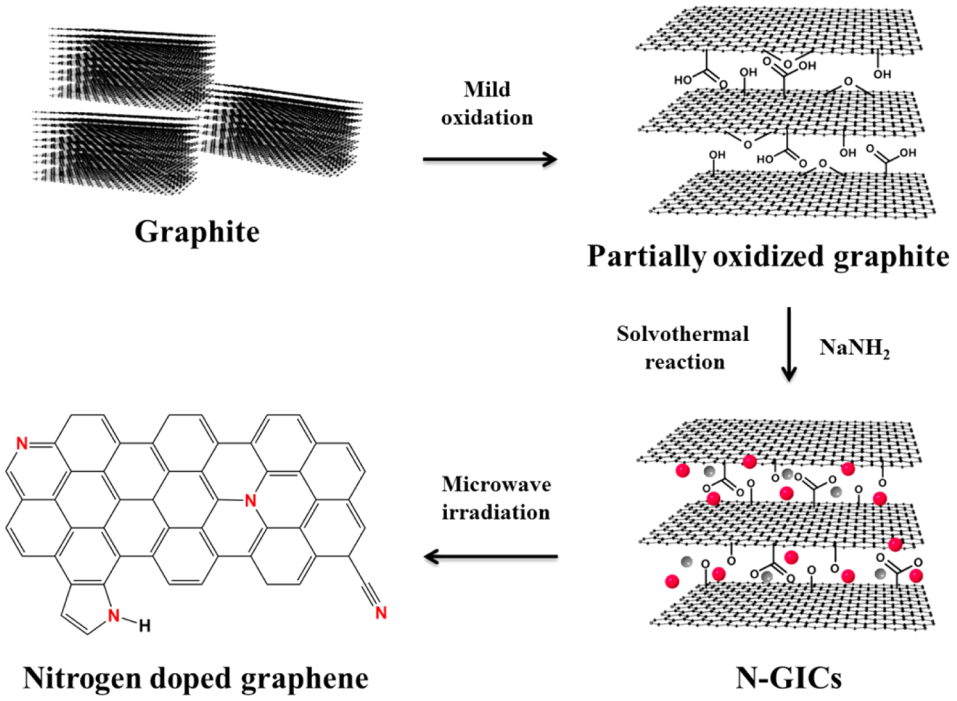

Figure 1. Schematics of microwave-assisted graphene exfoliation and doping process from bulk graphite.

the difference between dielectric constants of solvent and reactant can provide significant enhancement in reaction rates. Furthermore, the microwave irradiation method is unique in providing scaled-up processes without suffering thermal gradient effects,[21−23] thus leading to industrially meaningful advancement in the large-scale synthesis of nanoscale materials.[24,25] The use of microwave irradiation have been demonstrated for the synthesis of functionalized graphene oxide (GO),[26,27] the restoration of graphene from GO[28,29] and the exfoliation of graphite-intercalation compounds (GICs).[30,31] At this point, it can be proposed that high energy state induced by dielectric heating under microwave irradiation would impart a graphitic basal plane to afford dopant molecules, yielding a direct conversion of graphite to N-graphene which has not been reported yet by microwave irradiation. We successfully achieved the N-doping of graphitic layer through the microwave irradiation and thoroughly investigated the dependencies of structural and electrical properties of N-graphene according to the microwave irradiation power.

2. EXPERIMENTAL SECTION

2.1. Materials. Graphite flakes (+100 mesh, Aldrich), sulfuric acid (95−97%, Aldrich), fuming nitric acid (>90%, Yakuri Chemical), and $NaNH_2$ (95%, Aldrich) were obtained from commercial sources and used as received.

2.2. Synthesis of N-Graphene. Graphite-intercalation compounds (GICs) were prepared from graphite according to a modification of the Hummers-Offeman method.[32] A mixture of 5g of graphite flakes and 150 mL of sulfuric acid were gently stirred in a round-bottom flask, and 50 mL of fuming nitric acid was added into the mixture. The mixture was vigorously stirred at room temperature for 24 h. Deionized water was then poured slowly into the mixture. The resulting mixture was washed using distilled water several times, followed by centrifugation and drying at 60 °C for 24 h to obtain GICs.

The resulting GICs (0.5 g) was added to $NaNH_2$ (2 g), and the resulting mixture was transferred to a Teflon-lined autoclave (50 mL) filled with benzene up to 90% of the total volume, which was then sealed and maintained at 180 °C for 12 h. After natural cooling to room temperature, the as-synthesized products were washed thoroughly with distilled water several times, and centrifuged with ethanol and acetone, yielding nitrogen-containing GICs (N-GICs). To prepare N-graphene from N-GICs by irradiation, 0.5 g of N-GICs was sealed in a quartz vessel, which was fitted with a pressure and temperature probe. The quartz vessel was then placed on a turntable for uniform heating in microwave irradiation equipment (Anton Paar, Synthos-3000) at a frequency of 2.45 GHz. Irradiation power and exposure time were controlled, and temperature was monitored. The power was applied for 30 s, which was repeated for 2 times in the whole process.

For comparison, undoped graphene was prepared from the GICs by microwave irradiation. Overall reaction scheme and condition of N-graphene were applied except to remove mixing GICs with $NaNH_2$.

2.4. Characterization. The morphologies of undoped graphene and N-graphene samples were characterized by transmission electron microscopy (TEM) using a Hitachi-2100 TEM facility with accelerating voltage of 200 kV. TEM samples were prepared by drying a droplet of the graphene or N-graphene suspensions on a Cu grid with carbon film. Additionally, Atomic force microscopy (AFM) images were obtained to examine topology and thickness changes during irradiation, using MFP3D microscope (Asylum Research). The field emission scanning electron microscopy (FE-SEM) measurements were performed by using a JEOL JSM-6701F facility. An X-ray powder diffractometer (XRD, Shimadzu, X-6000, Cu Kα radiation) was used to determine the phase purity and crystallization degree. Room-temperature Raman spectra were recorded using a Renishaw InVia micro-Raman system with an excitation wavelength of 514 nm. X-ray photoelectron spectroscopy (XPS) analyses were carried out on a Thermo Fisher X-ray photoelectron spectrometer system. All spectra were taken using an Al K microfocused monochromatized source (1486.6 eV) with resolution of 0.6 eV. Electrical conductivity was measured by a four-point-probe measurement system (Napson, CRESBOX).

2.5. Electrode Preparation and Electrochemical Experiment. For three-electrode systems, the test electrode was prepared by loading slurry consisting of 95 wt % active materials, and 5 wt % polyvinylidene fluoride (PVDF) binder was fabricated using N-methyl pyrolidone (NMP) as a solvent. The slurry of the above mixture was subsequently pressed onto nickel foam, serving as the current collector. The prepared electrode was placed in a vacuum drying oven at 120 °C for 24 h. In the three-electrode system, the sample was used as the test electrode, coiled platinum as the counter electrode, Hg/HgO electrode (in 6 M KOH) or

dx.doi.org/10.1021/am405735c | ACS Appl. Mater. Interfaces 2014, 6, 6361−6368

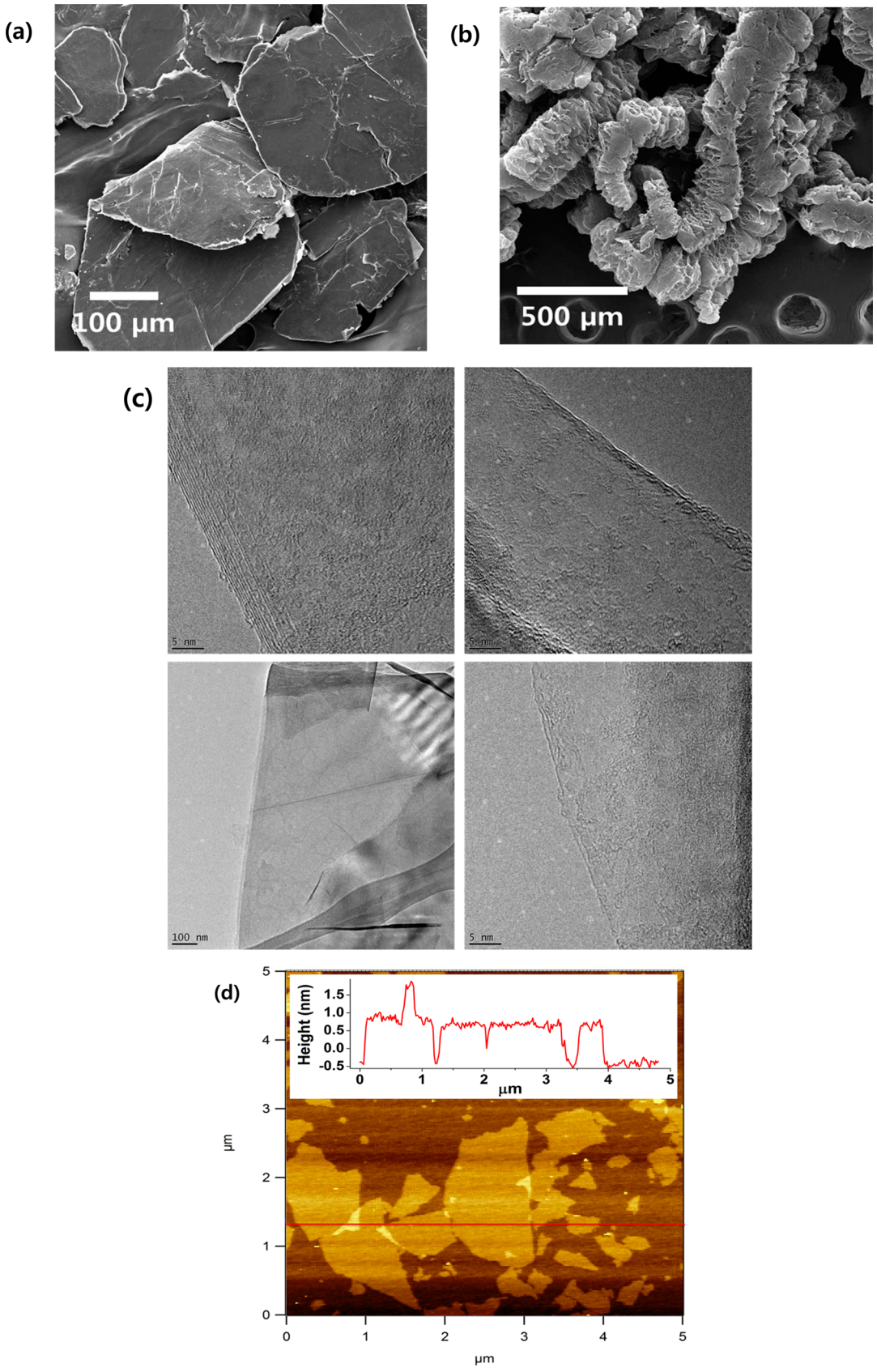

Figure 2. FE-SEM images of N-GICs (a) before and (b) after microwave irradiation. (c) TEM image of the highly exfoliated N-graphene and (d) AFM image of N-graphene after extreme delamination.

a saturated calomel electrode (SCE) (in 1 M H_2SO_4) as reference electrode. The electrochemical properties and capacitance measurements of the samples were examined by cyclic voltammetry (CV) and galvanostatic charge/discharge (chronopotentiometry) on an Autolab

dx.doi.org/10.1021/am405735c | *ACS Appl. Mater. Interfaces* 2014, 6, 6361−6368

PGSTAT-128N potentiostat/galvanostat. Galvanostatic cycling of supercapacitor electrodes was performed at a constant current of 0.5 A/g. The gravimetric specific capacitance, C_{sp} (F/g) was calculated from galvanostatic discharge curve as seen in eq 1

$$C_{sp} = I\Delta t/m\Delta V \quad (1)$$

where I (A) is applied constant current density, Δt is the discharge time (s), m (g) is the mass of carbon in each electrode, and ΔV (V) is the potential window. The geometric surface area of the electrodes was kept close to 1.0 cm^2. The active materials in the electrodes had a mass range of 1−3 mg/cm^2.

3. RESULTS AND DISCUSSION

The preparation of N-graphene was performed under microwave irradiation, as schematically illustrated in Figure 1. First, intercalation of graphite by a mixture of sulfuric and nitric acid produced GICs, which transformed to N-GICs by the solvothermal reaction with $NaNH_2$ in benzene. N-graphene was then prepared by microwave-heating of N-GICs under N_2 atmosphere. It was demonstrated that graphene can absorb microwave easily and reach to very high temperature in few seconds, quickly incorporating nitrogen atoms. $NaNH_2$ was chosen as a nitrogen source for doping as well as expansion−reducing agent because of the abundance of nitrogen and lower melting point of alkali amides. Thermal degradation of sodium amide at high temperature results in evolution of substantial quantities of gaseous nitrogen such as sodium nitride and ammonia, resulting in promotion of expansion along the *c*-axis direction.[33,34] Sonication further resulted in fragmentation of the already loose graphite layers to graphene nanosheets of mono- and few layers.

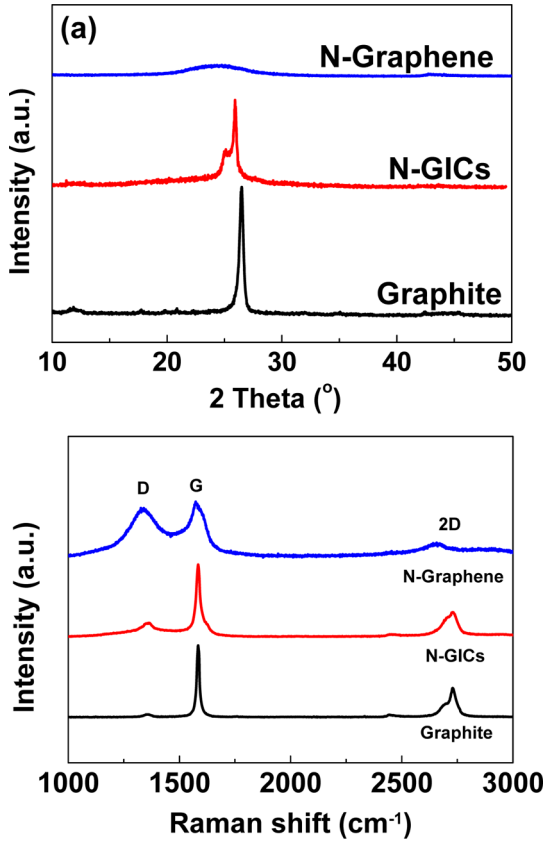

Figure 3. (a) XRD patterns and (b) Raman spectra of pristine graphite, N-GICs, and N-graphene.

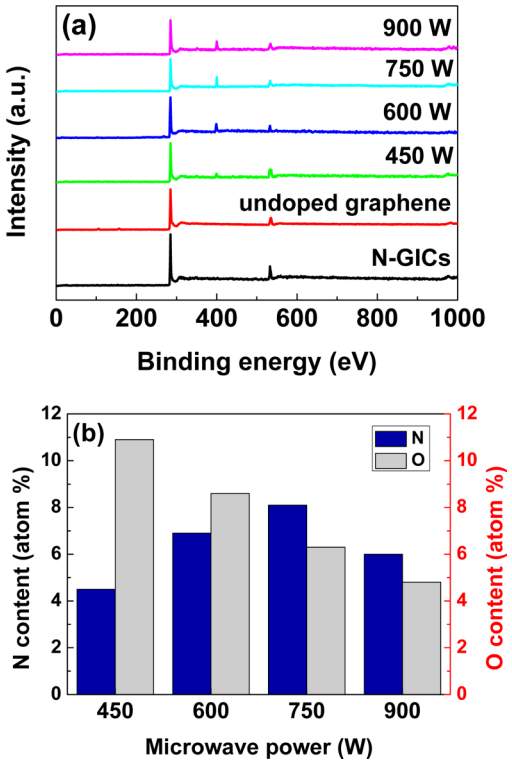

Figure 4. (a) XPS spectra of N-GICs, undoped graphene, and N-graphene obtained at various microwave power, and (b) contents of nitrogen and oxygen atoms of the respective N-graphene.

The average particle size and morphology of the N-GICs and N-graphene were observed by FE-SEM. The N-GICs before microwave irradiation has a relatively smooth surface and some small flakes were observed on the surface of the GICs as shown in Figure 2a. The flake shape of the GICs was irregular, similar to that of natural graphite. The mean diameter and thickness of the GICs before expansion were about 250 and 3 μm, respectively. After microwave irradiation, the accordion-like expanded structure of graphite was observed (Figure 2b). The FE-SEM image at high magnification shows layered structures with thicknesses ranging from a few nanometers to a few micrometers. To further characterize the graphene sheets, TEM analysis was conducted. As shown in Figure 2c the TEM images indicate that those nanosheets mainly consist of single to few layers. With small quantity of monolayer graphene nanosheets, a larger proportion of flakes were few-layer graphene, including some bilayers and trilayers. Furthermore, AFM analysis in Figure 2d shows that the minimum thickness is about 1.2 nm for N-graphene sheets, and most of nanosheets have a thickness of 1−3.5 nm (see Figure S1 in the Supporting Information), further confirming the formation of few-layer graphene structure.[19,35,36] The thickness is somewhat larger than that of flat defect-free graphene due to the presence of oxygen-containing functional groups and structural defects which impart topological roughness to N-graphene sheets. The lateral dimension is in the range of several hundred nanometers to several micrometers.

The XRD patterns of graphite, N-GICs and N-graphene are shown in Figure 3a. The patterns of N-GICs seems to be similar to that of the bulk graphite (d-spacing of 0.335 nm at 2θ = 26.41°), but additional peaks appear at 25.12° and graphite peak was shifted to lower angle, 25.92°. These two peaks evolution coupled with peak shift indicate successful intercalation to GICs

dx.doi.org/10.1021/am405735c | ACS Appl. Mater. Interfaces 2014, 6, 6361−6368

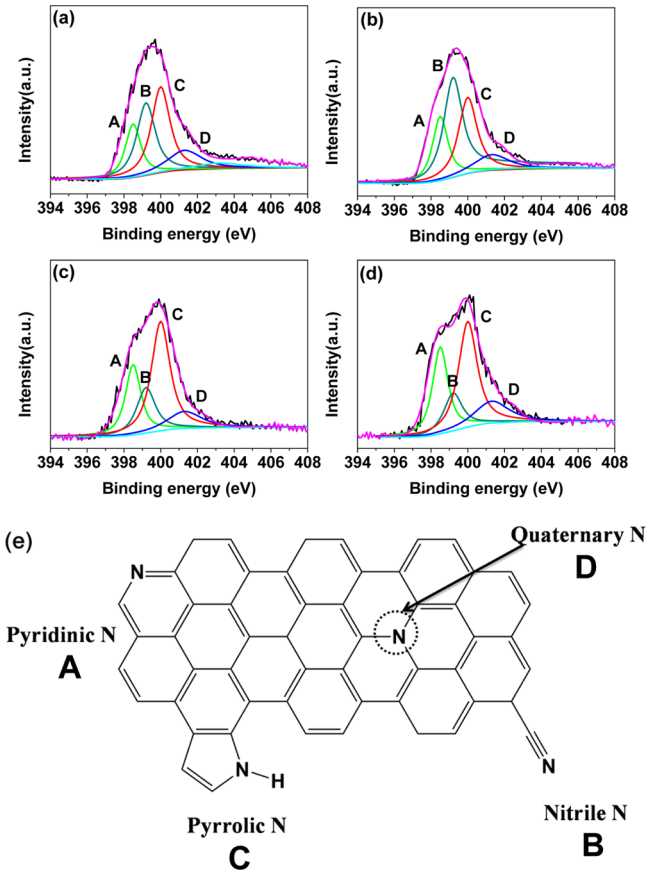

Figure 5. N1s XPS spectra of N-graphene at (a) 450, (b) 600, (c) 750, and (d) 900 W of microwave irradiation power. (e) Schematic of postulated nitrogenation on a graphitic layer.

from densely stacked graphitic layers of bulk graphite. After microwave irradiation, the sharp peak near 26.41° for graphite and N-GICs completely disappeared, whereas a weak and broad diffraction peak around 25° was observed, which is a typical evidence for the exfoliation of graphite to few-layer graphene. The microwave-assisted N-graphene formation could be also supported by Raman analysis, as can be seen in Figure 3b. While graphite and N-GICs showed less intensive D peak at 1350 cm^{-1} and higher intensity of G peak at 1580 cm^{-1},[37] N-graphene presented relatively high intensity of D peak, lower intensity of G peak converged with newly observed D′ peak, which located at the 1620 cm^{-1}, which originate from a double resonance (DR) Raman scattering process.[38,39] Also, it is notable that there is an abrupt broadening and decrease of 2D band imparted by microwave irradiation under $NaNH_2$ for N-doping, indicating that the disorder increases[40,41] with the microwave treatment. As reported previously,[42,43] the evolution of Raman spectra of graphene layer in this manner can be interpreted that there is a distortion of graphitic crystal structure, which is correlated with the incorporation of heterogeneous nitrogen atom into the graphene layers.

The bonding configuration of doped nitrogen and the surface composition of corresponding nitrogen-containing chemical structures were examined using XPS. Figure 4 shows that the overall nitrogen content in N-graphene changes with microwave irradiation power. The peaks at about 284, 401, and 534 eV can be assigned to the binding energy of C1s, N1s, and O1s, respectively. The XPS spectra of N-GICs as well as undoped graphene indicate that the nanosheets contain ca. 20.8% of oxygen and no signal concerning nitrogen could be detected, and the presence of nitrogen was detected only when irradiation was given with $NaNH_2$ intercalated. As shown in Figure 4 (see Table S1 in the Supporting Information), N-doping occurred at irradiation power as low as 450 W for N-GICs, with ∼4.5% of nitrogen detected in the sample. When irradiation power was varied from 450 to 900 W, atomic content of nitrogen in N-graphene was found in a range of 4−8%, with 750 W irradiation power affording the highest N-doping level of ∼8.1%, which is a notable result when compared with the reported value in the literature (see Table S2 in the Supporting Information). Moreover, it is notable that the atomic content of oxygen was dropped from 20.8% for N-GICs to 4.8% for NG-900 (the N-graphene prepared at 900 W of irradiation power), indicating that oxygen-containing functional groups were effectively removed during microwave irradiation. This is due to the formation of C−N bonds and the recovery to sp^2 graphitic lattice of defected GICs by microwave irradiation with $NaNH_2$. Along with simple and fast process, the microwave-assisted N-doping process has the additional advantage capable of direct conversion of graphite to N-doped graphene with much lower defect and oxygen content compared to other methods reported to date.

To evaluate the bonding configuration and chemical states of doped nitrogen atoms, we examined the high-resolution N1s XPS spectra of N-graphene; the results are shown in Figure 5. Generally, there are several N-containing functional groups in N-doped graphene, which can be identified by the bonding configurations of nitrogen atom. These groups include pyridinic N at 398.5 eV(peak A), nitrile N at 399.3 eV(peak B), pyrrolic N at 400.1 eV(peak C), and quaternary N at 401.3 eV(peak D).[13,44] As can be seen in Figure 5e, pyridinic N refers to N atoms at the edges of graphene planes, where each N atom is bonded to two carbon atoms and donates one p-electron to the aromatic π system and nitrile N atoms are C triple bonded to N with a lone pair on the N. Pyrrolic N atoms are incorporated into five membered heterocyclic rings, which are bonded to two carbon atoms and contribute two p-electrons to the π system and quaternary N, which is also called "graphitic N" or "substituted *N*", is incorporated into the graphene layer and substitute carbon atoms within the graphene plane. Based on the XPS results in Figure 4a−d, the change of content of the N species with different microwave power can be traced as follows; as the microwave power increases, the intensities of the pyridinic N and pyrrolic N peaks increase, while the intensity of nitrile N peak decreases. This phenomenon can be interpreted that when the radiation power increases, the intramolecular dehydration or

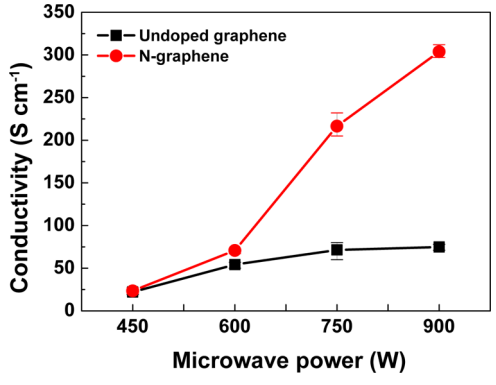

Figure 6. Electrical conductivity changes of N-graphene and undoped graphene by control of microwave irradiation power.

dx.doi.org/10.1021/am405735c | *ACS Appl. Mater. Interfaces* 2014, 6, 6361−6368

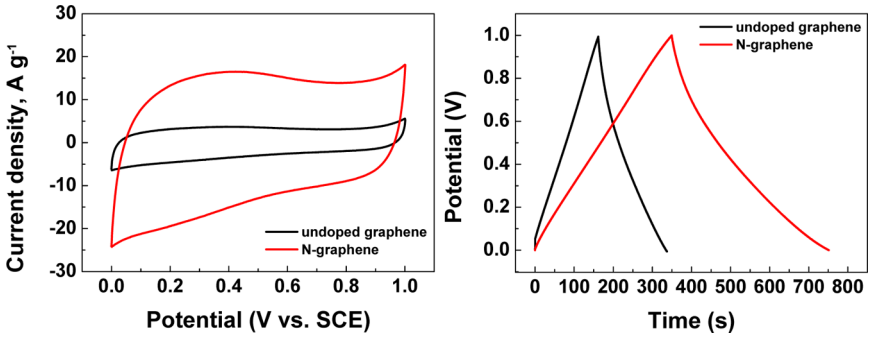

Figure 7. Electrochemical performances of undoped graphene and N-graphene (NG-900) when used as an electrode in 1 M H_2SO_4 solution: (a) CV diagrams obtained at scan rate of 50 mV/s, (b) galvanostatic charge/discharge curves at a current density of 0.5 A/g.

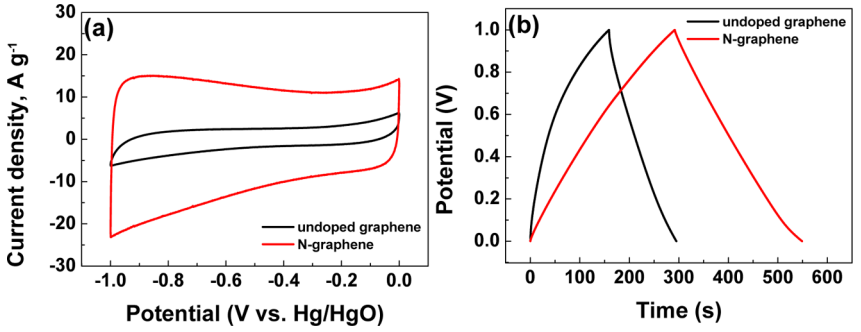

Figure 8. Electrochemical performances of undoped graphene and N-graphene (NG-900) when used as an electrode in 6 M KOH solution: (a) CV diagrams obtained at scan rate of 50 mV/s, (b) galvanostatic charge/discharge curves at a current density of 0.5 A/g.

decarbonylation take place to generate thermally stable heterocyclic aromatic moieties such as pyridine, pyrrole and quaternary type N sites. It is noteworthy that N-doping takes place at basal planes and edges simultaneously, which is different from previous reports[9,45] that N-doping would take place mainly at edges because of the higher reactivity. The result indicates that higher microwave power would favor the formation of pyridinic N in the graphene sheets, whereas the lower microwave power would lead to more incorporation of N in terms of nitrile N, and larger portion of pyrrolic N, regardless of microwave power.

To evaluate the property change of graphene imparted by microwave irradiation assisted N-doping, the electrical conductivities of N-graphene as well as undoped graphene (obtained from the microwave treatment of the GIC without nitrogen source) were examined. As can be seen in Figure 6, N-graphene shows notable enhancement of electrical conductivity compared with undoped graphene. The NG-900 showed the highest conductivity among all the N-graphene species, approximately 305 S cm^{-1}, because of the increasing sp^2 carbon networks, decreasing oxygen content, as well as defects associated with incorporation of nitrogen atom. On the other hand, when the irradiation power was not so high, such as the case of NG-450, very low conductivity was found, possibly because of the incomplete restoration of sp^2 carbon networks from oxidized graphitic layer formed during the harsh oxidative expansion process of graphite. The conductivity data, in conjunction with XPS result, reveal that conductivity of N-graphene increased with increasing C/O ratio, which could be attributed to the degree of restoring the sp^2 carbon networks in N-GICs during the microwave irradiation processes.

In the case of graphene-based supercapacitor application, many researchers recently focused on the effect of doping materials on the electrochemical properties of graphene-based electrodes. Thus, we investigated the electrochemical properties of N-graphene by microwave irradiation using cyclic voltammetry (CV) and galvanostatic charge/discharge in acidic (1 M H_2SO_4) and basic (6 M KOH) media with three-electrode system.

As shown in Figures 7 and 8, the NG-900 electrode exhibits a much higher current density than that of undoped graphene, indicating a greatly increased capacitance due to the N-doping and efficient exfoliation from nitrogen-containing intercalants. As confirmed by XPS, NG-900 includes large amount of pyridinic and pyrrolic N moieties, which provides a pair of electrons introducing electron donor properties to the layer.[46] These nitrogen species are located at the easily accessible edges of graphene layers, and therefore they can easily contribute to the total capacitance with the pseudocapacitive effect.[47,48] Furthermore, quaternary nitrogen groups have enhancing effects on the capacitance due to their positive charge and thus an improved electron transfer through the carbon surface.[49] Large surface area (~240 m^2/g) from N-doped graphene could additionally result in high capacitances compared with that of undoped graphene sample (~125 m^2/g). (Figure S2 and Table S3 in Supporting Information) The specific capacitance, C_{sp} of the electrode material was calculated from galvanostatic discharge curves. It was obtained that C_{sp} for NG-900 is 200 F/g in 1 M H_2SO_4, and 130 F/g in 6 M KOH at a current density of 0.5 A/g, which is significantly larger than that of undoped graphene, 87 F/g in 1 M H_2SO_4, and 70 F/g in 6 M KOH at 0.5 A/g. The supercapacitive performances in acidic electrolyte (Figure 7) are better than in basic electrolyte (Figure 8), which is related that pseudocapacitive properties of pyridinic and pyrrolic N moieties more activates in acidic conditions.[50]

dx.doi.org/10.1021/am405735c | ACS Appl. Mater. Interfaces 2014, 6, 6361−6368

4. CONCLUSION

We have demonstrated a facile microwave irradiation approach to prepare nitrogen-doped graphene from bulk graphite. The control of irradiation power and addition of nitrogen source are capable of changing the atomic contents of nitrogen in graphene layers up to 8.1%, resulting in notable enhancement of electrical conductivity upon nitrogen doping. It is also noted that the nitrogen-doped graphene shows higher specific capacitance than that of undoped graphene, the maximum specific capacitance of 200 F/g can be obtained. The enhancement of capacitive performance can attribute to the pseudocapacitive effect based on the nitrogen doping for graphene. It was proved that the microwave irradiation-assisted doping method for graphene significantly reduces the doping reaction time, cost, and energy required, compared to the conventional solution-based methods, and it would be highly beneficial to the preparation of heteroatom-doped graphene, especially in large scale.

■ ASSOCIATED CONTENT

Ⓢ Supporting Information

AFM images analysis and surface area measurements of the N-doped graphene. This material is available free of charge via the Internet at http://pubs.acs.org.

■ AUTHOR INFORMATION

Corresponding Author

*E-mail: s-slee@kist.re.kr.

Notes

The authors declare no competing financial interest.

■ ACKNOWLEDGMENTS

This work was kindly supported by a grant (Code 2011-0032156) from the Center for Advanced Soft Electronics under the Global Frontier Research Program of the Ministry of Science, ICT & Future Planning, Korea, and the R&D program for the technology of World Premier Materials by the Ministry of Trade, Industry and Energy, Korea, as well as the internal project of KIST. S.-S. Lee also appreciates the research grant from the KU-KIST Graduate School.

■ REFERENCES

(1) Ponomarenko, L. A.; Schedin, F.; Katsnelson, M. I.; Yang, R.; Hill, E. W.; Novoselov, K. S.; Geim. Chaotic Dirac Billiard in Graphene Quantum Dots. A. K. *Science* **2008**, *320*, 356−358.

(2) Lu, J.; Drzal, L. T.; Worden, R. M.; Lee, I. Simple Fabrication of a Highly Sensitive Glucose Biosensor Using Enzymes Immobilized in Exfoliated Graphite Nanoplatelets Nafion Membrane. *Chem. Mater.* **2007**, *19*, 6240−6246.

(3) Schwierz, F. Graphene Transistors. *Nat. Nanotechnol.* **2010**, *5*, 487−496.

(4) Dimitrakakis, G. K.; Tylianakis, E.; Froudakis, G. E. Pillared Graphene: A New 3D Network Nanostructure for Enhanced Hydrogen Storage. *Nano Lett.* **2008**, *8*, 3166−3170.

(5) Lightcap, I. V; Kosel, T. H.; Kamat, P. V. Anchoring Semiconductor and Metal Nanoparticles on a Two-Dimensional Catalyst Mat. Storing and Shuttling Electrons with Reduced Graphene Oxide. *Nano Lett.* **2010**, *10*, 577−583.

(6) Cervantes-Sodi, F.; Csányi, G.; Piscanec, S.; Ferrari, A. C. Edge-Functionalized and Substitutionally Doped Graphene Nanoribbons: Electronic and Spin Properties. *Phys. Rev. B* **2008**, *77*, 165427.

(7) Song, L. L.; Zheng, X. H.; Wang, R. L.; Zeng, Z. Dangling Bond States, Edge Magnetism, and Edge Reconstruction in Pristine and B/N-Terminated Zigzag Graphene Nanoribbons. *J. Phys. Chem. C* **2010**, *114*, 12145−12150.

(8) Dutta, S.; Pati, S. K. Novel Properties of Graphene Nanoribbons: a Review. *J. Mater. Chem.* **2010**, *20*, 8207−8223.

(9) Wang, X.; Li, X.; Zhang, L.; Yoon, Y.; Weber, P. K.; Wang, H.; Guo, J.; Dai, H. N-Doping of Graphene Through Electrothermal Reactions with Ammonia. *Science* **2009**, *324*, 768−771.

(10) Panchakarla, L. S.; Subrahmanyam, K. S.; Saha, S. K.; Govindaraj, A.; Krishnamurthy, H. R.; Waghmare, U. V; Rao, C. N. R. Synthesis, Structure, and Properties of Boron- and Nitrogen-Doped Graphene. *Adv. Mater.* **2009**, *21*, 4726−4730.

(11) Gong, K.; Du, F.; Xia, Z.; Durstock, M.; Dai, L. Nitrogen-Doped Carbon Nanotube Arrays with High Electrocatalytic Activity for Oxygen Reduction. *Science* **2009**, *323*, 760−764.

(12) Lee, S. U.; Belosludov, R. V; Mizuseki, H.; Kawazoe, Y. Designing Nanogadgetry for Nanoelectronic Devices with Nitrogen-Doped Capped Carbon Nanotubes. *Small* **2009**, *5*, 1769−1775.

(13) Reddy, A. L. M.; Srivastava, A.; Gowda, S. R.; Gullapalli, H.; Dubey, M.; Ajayan, P. M. Synthesis Of Nitrogen-Doped Graphene Films For Lithium Battery Application. *ACS Nano* **2010**, *4*, 6337−6342.

(14) Zhang, L.-S.; Liang, X.-Q.; Song, W.-G.; Wu, Z.-Y. Identification of the Nitrogen Species on N-Doped Graphene Layers and Pt/NG Composite Catalyst for Direct Methanol Fuel Cell. *Phys. Chem. Chem. Phys.* **2010**, *12*, 12055−12059.

(15) Liu, Q.; Cui, Z.-M.; Ma, Z.; Bian, S.-W.; Song, W.-G. Highly Active and Stable Material for Catalytic Hydrodechlorination Using Ammonia-Treated Carbon Nanofibers as Pd Supports. *J. Phys. Chem. C* **2008**, *112*, 1199−1203.

(16) Wang, X.; Lee, J. S.; Zhu, Q.; Liu, J.; Wang, Y.; Dai, S. Ammonia-Treated Ordered Mesoporous Carbons as Catalytic Materials for Oxygen Reduction Reaction. *Chem. Mater.* **2010**, *22*, 2178−2180.

(17) Li, N.; Wang, Z.; Zhao, K.; Shi, Z.; Gu, Z.; Xu, S. Large Scale Synthesis of N-Doped Multi-Layered Graphene Sheets by Simple Arc-Discharge Method. *Carbon* **2010**, *48*, 255−259.

(18) Lin, Y.-C.; Lin, C.-Y.; Chiu, P.-W. Controllable Graphene N-Doping with Ammonia Plasma. *Appl. Phys. Lett.* **2010**, *96*, 133110−133113.

(19) Li, X.; Wang, H.; Robinson, J. T.; Sanchez, H.; Diankov, G.; Dai, H. Simultaneous Nitrogen Doping and Reduction of Graphene Oxide. *J. Am. Chem. Soc.* **2009**, *131*, 15939−44.

(20) Wakeland, S.; Martinez, R.; Grey, J. K.; Luhrs, C. C. Production of Graphene from Graphite Oxide using Urea as Expansion−Reduction Agent. *Carbon* **2010**, *48*, 3463−3470.

(21) Muraliganth, T.; Stroukoff, K. R.; Manthiram, A. Microwave-Solvothermal Synthesis of Nanostructured Li2MSiO4/C (M = Mn and Fe) Cathodes for Lithium-Ion Batteries. *Chem. Mater.* **2010**, *22*, 5754−5761.

(22) Yoon, S.; Manthiram, A. Microwave-Hydrothermal Synthesis of W0. 4Mo0.6O3 and Carbon-Decorated WOx-MoO2 Nanorod Anodes for Lithium Ion Batteries. *J. Mater. Chem.* **2011**, *21*, 4082−4085.

(23) Gerbec, J. A.; Magana, D.; Washington, A.; Strouse, G. F. Microwave-Enhanced Reaction Rates for Nanoparticle Synthesis. *J. Am. Chem. Soc.* **2005**, *127*, 15791−15800.

(24) Panda, A. B.; Glaspell, G.; El-Shall, M. S. Microwave Synthesis of Highly Aligned Ultra Narrow Semiconductor Rods and Wires. *J. Am. Chem. Soc.* **2006**, *128*, 2790−2791.

(25) Nadagouda, M. N.; Speth, T. F.; Varma, R. S. Microwave-Assisted Green Synthesis of Silver Nanostructures. *Acc. Chem. Res.* **2011**, *44*, 469−478.

(26) Melucci, M.; Treossi, E.; Ortolani, L.; Giambastiani, G.; Morandi, V.; Klar, P.; Casiraghi, C.; Samori, P.; Palermo, V. Facile Covalent Functionalization of Graphene Oxide Using Microwaves: Bottom-up Development of Functional Graphitic Materials. *J. Mater. Chem.* **2010**, *20*, 9052−9060.

(27) Economopoulos, S. P.; Rotas, G.; Miyata, Y.; Shinohara, H.; Tagmatarchis, N. Exfoliation and Chemical Modification Using Microwave Irradiation Affording Highly Functionalized Graphene. *ACS Nano* **2010**, *4*, 7499−7507.

(28) Li, Z.; Yao, Y.; Lin, Z.; Moon, K.-S.; Lin, W.; Wong, C. Ultrafast, Dry Microwave Synthesis of Graphene Sheets. *J. Mater. Chem.* **2010**, *20*, 4781−4783.

(29) Chen, W.; Yan, L.; Bangal, P. R. Preparation of Graphene by the Rapid and Mild Thermal Reduction of Graphene Oxide Induced by Microwaves. *Carbon* **2010**, *48*, 1146−1152.
(30) Wei, T.; Fan, Z.; Luo, G.; Zheng, C.; Xie, D. Rapid and Efficient Method to Prepare Exfoliated Graphite by Microwave Irradiation. *Carbon* **2009**, *47*, 337−339.
(31) Park, S.-H.; Bak, S.-M.; Kim, K.-H.; Jegal, J.-P.; Lee, S.-I.; Lee, J.; Kim, K.-B. Solid-State Microwave Irradiation Synthesis of High Quality Graphene Nanosheets under Hydrogen Containing Atmosphere. *J. Mater. Chem.* **2011**, *21*, 680−686.
(32) Hummers, W.; Offeman, R. E. Preparation of Graphitic Oxide. *J. Am. Chem. Soc.* **1958**, *80*, 1339.
(33) Fijalkowski, K. J.; Grochala, W. Substantial Emission of NH_3 during Thermal Decomposition of Sodium Amidoborane, $NaNH_2BH_3$. *J. Mater. Chem.* **2009**, *19*, 2043−2050.
(34) Schniepp, H. C.; Li, J.-L.; McAllister, M. J.; Sai, H.; Herrera-Alonso, M.; Adamson, D. H.; Prud'homme, R. K.; Car, R.; Saville, D. A.; Aksay, I. A. Functionalized Single Graphene Sheets Derived from Splitting Graphite Oxide. *J. Phys. Chem. B* **2006**, *110*, 8535−8539.
(35) McAllister, M. J.; Li, J.-L.; Adamson, D. H.; Schniepp, H. C.; Abdala, A. A.; Liu, J.; Herrera-Alonso, M.; Milius, D. L.; Car, R.; Prud'homme, R. K.; Aksay, I. A. Single Sheet Functionalized Graphene by Oxidation and Thermal Expansion of Graphite. *Chem. Mater.* **2007**, *19*, 4396−4404.
(36) Mkhoyan, K. A.; Contryman, A. W.; Silcox, J.; Stewart, D. A.; Eda, G.; Mattevi, C.; Miller, S.; Chhowalla, M. Atomic and Electronic Structure of Graphene-Oxide. *Nano Lett.* **2009**, *9*, 1058−1063.
(37) Ferrari, A. C.; Meyer, J. C.; Scardaci, V.; Casiraghi, C.; Lazzeri, M.; Mauri, F.; Piscanec, S.; Jiang, D.; Novoselov, K. S.; Roth, S.; Geim, A. K. Raman Spectrum of Graphene and Graphene Layers. *Phys. Rev. Lett.* **2006**, *97*, 187401.
(38) Thomsen, C.; Reich, S. Double Resonant Raman Scattering in Graphite. *Phys. Rev. Lett.* **2000**, *85*, 5214−5217.
(39) Saito, R.; Jorio, A.; Souza Filho, A. G.; Dresselhaus, G.; Dresselhaus, M. S.; Pimenta, M. A. Probing Phonon Dispersion Relations of Graphite by Double Resonance Raman Scattering. *Phys. Rev. Lett.* **2001**, *88*, 27401.
(40) Guo, B.; Liu, Q.; Chen, E.; Zhu, H.; Fang, L.; Gong, J. Controllable N-Doping of Graphene. *Nano Lett.* **2010**, *10*, 4975−4980.
(41) Park, S. H.; Chae, J.; Cho, M.-H.; Kim, J. H.; Yoo, K.-H.; Cho, S. W.; Kim, T. G.; Kim, J. W. High Concentration of Nitrogen Doped into Graphene using N_2 Plasma with an Aluminum Oxide Buffer Layer. *J. Mater. Chem. C* **2014**, *2*, 933−939.
(42) Tuinstra, F.; Koenig, J. L. Raman Spectrum of Graphite. *J. Chem. Phys.* **1970**, *53*, 1126−1130.
(43) McCulloch, D. G.; Prawer, S.; Hoffman, A. Structural Investigation of Xenon-Ion-Beam-Irradiated Glassy Carbon. *Phys. Rev. B* **1994**, *50*, 5905−5917.
(44) Casanovas, J.; Ricart, J. M.; Rubio, J.; Illas, F.; Jiménez-Mateos, J. M. Origin of the Large N 1s Binding Energy in X-ray Photoelectron Spectra of Calcined Carbonaceous Materials. *J. Am. Chem. Soc.* **1996**, *118*, 8071−8076.
(45) Arrigo, R.; Hävecker, M.; Wrabetz, S.; Blume, R.; Lerch, M.; McGregor, J.; Parrott, E. P. J.; Zeitler, J. A.; Gladden, L. F.; Knop-Gericke, A.; Schlögl, R.; Su, D. S. Tuning the Acid/Base Properties of Nanocarbons by Functionalization via Amination. *J. Am. Chem. Soc.* **2010**, *132*, 9616−9630.
(46) Deng, D.; Pan, X.; Yu, L.; Cui, Y.; Jiang, Y.; Qi, J.; Li, W.-X.; Fu, Q.; Ma, X.; Xue, Q.; Sun, G.; Bao, X. Toward N-Doped Graphene via Solvothermal Synthesis. *Chem. Mater.* **2011**, *23*, 1188−1193.
(47) Xu, J.; Wang, K.; Zu, S.-Z.; Han, B.-H.; Wei, Z. Hierarchical Nanocomposites of Polyaniline Nanowire Arrays on Graphene Oxide Sheets with Synergistic Effect for Energy Storage. *ACS Nano* **2010**, *4*, 5019−5026.
(48) Liu, R.; Duay, J.; Lane, T.; Bok Lee, S. Synthesis and Characterization of RuO_2/Poly(3,4-ethylenedioxythiophene) Composite Nanotubes for Supercapacitors. *Phys. Chem. Chem. Phys.* **2010**, *12*, 4309−4316.
(49) Hulicova-Jurcakova, D.; Seredych, M.; Lu, G. Q.; Bandosz, T. J. Combined Effect of Nitrogen- and Oxygen-Containing Functional Groups of Microporous Activated Carbon on its Electrochemical Performance in Supercapacitors. *Adv. Funct. Mater.* **2009**, *19*, 438−447.
(50) Zhu, H.; Wang, X.; Yang, F.; Yang, X. Promising Carbons for Supercapacitors Derived from Fungi. *Adv. Mater.* **2011**, *23*, 2745−2748.